JGR Atmospheres

RESEARCH ARTICLE
10.1029/2021JD034932

Compact Lightning Strokes in Winter Thunderstorms

Ting Wu[1], **Daohong Wang**[1], **and Nobuyuki Takagi**[1]

[1]Department of Electrical, Electronic and Computer Engineering, Gifu University, Gifu, Japan

Key Points:

- Lightning strokes with extremely short (on average 300 m) channels are identified and are named as compact strokes
- Compact strokes are mainly produced in small gaps between mountain tops and negative charge regions in winter thunderstorms
- Compact strokes start with a fast downward negative leader followed by a return stroke that is largely different from normal return strokes

Supporting Information:

Supporting Information may be found in the online version of this article.

Correspondence to:

T. Wu,
tingwu@gifu-u.ac.jp

Citation:

Wu, T., Wang, D., & Takagi, N. (2021). Compact lightning strokes in winter thunderstorms. *Journal of Geophysical Research: Atmospheres*, *126*, e2021JD034932. https://doi.org/10.1029/2021JD034932

Received 18 MAR 2021
Accepted 16 JUL 2021

Abstract With the observation of a 14-site Fast Antenna Lightning Mapping Array in the Hokuriku region of Japan, we identified a special type of lightning stroke called "compact stroke" in winter thunderstorms. A compact stroke starts with a fast downward negative leader followed by a "compact return stroke." Compact strokes have the following characteristics that are not seen in normal lightning strokes: (a) Durations of preceding discharges (defined as the time difference between the return stroke and the start of the flash) are generally smaller than 200 μs. (b) Most compact strokes are inferred to be produced in small gaps between mountain tops and negative charge regions in winter thunderstorms. (c) Channel lengths of compact strokes are estimated to be shorter than 600 m with an average of about 300 m. (d) Characteristics of electric field change waveforms of compact return strokes are closely related with durations of preceding discharges. (e) Peak currents of compact return strokes increase with increasing channel lengths. It seems that elevations of mountain surfaces where compact strokes occur are comparable to the altitude of the lower positive charge region, so we speculate that the mountain surface and the near-surface space carry positive charges when a storm is overhead and are virtually the lower positive charge region of a normal tripole structure. As a result, compact strokes are confined between the main negative and lower positive charge regions, and small pulses with short durations preceding compact return strokes are produced by downward negative leaders corresponding to the preliminary breakdown stage.

Plain Language Summary The return stroke in negative cloud-to-ground lightning flashes is the most well-studied discharge process in lightning and is the process responsible for most lightning-related damages. In this study, we report for the first time a special type of return stroke called "compact return stroke" in winter thunderstorms. Compact return strokes mostly occur in mountain areas and lower negative charges. Their channels are at least one order of magnitude shorter than those of normal return strokes. Their electric field change waveforms are distinctly different from those of normal return strokes, and unlike normal return strokes, their waveform characteristics are closely related with channel lengths. It is inferred that compact return strokes are produced in small gaps between mountain tops and negative charge regions in shallow winter thunderstorms.

1. Introduction

The return stroke (RS) is the most well-studied process in lightning (Rakov & Uman, 2003). The first RS in a negative cloud-to-ground (CG) flash is usually preceded by the preliminary breakdown (PB, also called initial breakdown) and the stepped leader, and the time difference between the start of a negative CG flash and the first RS is usually from several to a few tens of ms and occasionally hundreds of ms (Beasley et al., 1982; Clarence & Malan, 1957; Gomes et al., 1998; Kolmašová et al., 2014; Zhu et al., 2015). In winter, however, thunderclouds are much shallower and the time difference can be much shorter (Brook, 1992; Wu et al., 2013). For example, Wu et al. (2013) reported a negative CG flash with the time difference between the first RS and the start of the flash shorter than 1 ms.

Wu et al. (2014) further reported the so-called "large bipolar event" (LBE) in winter which was inferred to be a special type of RS not preceded by the PB and the stepped leader. LBEs only occurred on land so it was speculated that they were associated with tall grounded objects. However, the study of Wu et al. (2014) was based on the observation of a low-frequency (LF) lightning location system that was far away from the Japan Sea coast where LBEs were observed, so they could not get accurate location results of LBEs. Lightning discharges similar to LBEs have also been reported in other regions (Azadifar et al., 2019; Cummer et al., 2020). However, so far the physical mechanism of the LBE is still not well understood. Particularly, if

the LBE is a component of an upward lightning flash, it is difficult to explain why it produces a distinctive large bipolar waveform, and if the LBE is similar to the first stroke in a negative CG flash, it is difficult to explain why it is not preceded by the PB and the stepped leader.

During the winter of 2018–2019, we set up a new LF system called the Fast Antenna Lightning Mapping Array (FALMA) consisting of 14 sites in the Hokuriku region to observe winter lightning with close distances. Based on the FALMA observation, we will demonstrate in this paper the existence of a special type of RS that is not preceded by normal stepped leader processes. They are mainly produced in small gaps formed between mountain tops and negative charge regions in winter thunderclouds and are inferred to have very short channels. These special RSs are different from normal RSs in many respects, and we will name them as "compact RSs." A compact RS is preceded by a fast downward negative leader, and characteristics of the two processes are closely related with each other. For simplicity, we will call a compact RS along with its preceding negative leader as a "compact stroke." We will also demonstrate that the LBE reported by Wu et al. (2014) is a kind of compact RS.

2. Observation and Data

The FALMA is an LF lightning mapping system consisting of multiple observation sites with fast antennas as the sensor. The fast antenna has a time constant of 200 μs, and the electric field change (E-change) signals are recorded with a sampling rate of 10 MS/s and a pretrigger length of at least 500 ms during the winter observation. The FALMA is capable of three-dimensional lightning mapping with exceptional details (Wu et al., 2018). From November 2018 to March 2019, we carried out winter lightning observation in the Hokuriku region on the Japan Sea coast with a 14-site FALMA. Locations of these 14 sites are shown as black squares in Figure 1. For winter lightning observation, however, due to the fact that lightning discharges in winter occur at much lower altitudes and are much more complicated than those in summer, location accuracy of the FALMA in winter is much lower, especially for the height results (Wu et al., 2020a). Therefore, we will not use height results for the analysis of this paper.

The objective of this study is to identify special RSs such as LBEs that are not preceded by normal PB and stepped leader processes and are systematically different from normal RSs, but we will not limit our analysis to LBEs. We first use a very simple criteria to select possible special strokes: stroke-like large pulses with the duration of preceding discharges shorter than 1 ms. Specifically, any selected pulse has to meet the following criteria:

1. The time difference between the pulse and the start of the flash to which the pulse belongs is shorter than 1 ms.
2. The pulse is much larger (at least two times) than pulses before and after it.
3. The pulse has different waveforms with pulses before and after it. In other words, the pulse is not part of a pulse train. This is mainly to exclude occasional large PB pulses.
4. The pulse should be recorded by at least eight sites and is located in the region shown in Figure 1. This is to exclude RSs that occur very far away.

With these criteria, a total of 186 events that have the same polarity as negative RSs are identified. These events are represented by colored dots in Figure 1. Several events having the same polarity as positive RSs are also identified. However, as will be demonstrated in this paper, a large sample is needed to identify RSs that are truly different from normal RSs. Therefore, we will focus on negative events in this study. In Section 3.4, we will briefly analyze two positive events that may be special positive strokes. It is worth noting that all these identified special RSs are first RSs.

It should be noted that these selected events are "possible" special strokes which will be described in Section 3.1. We will further analyze these events in Section 3.2 and demonstrate that some of these events are systematically different from normal RSs. These events will be named as compact RSs. Compact RSs along with preceding leader processes will be called compact strokes. The most significant characteristic of compact strokes is the short channel, and in Section 3.3, we will estimate channel lengths of compact strokes.

Atmospheric electricity sign convention is used in this paper, so a negative RS produces the E-change waveform with an initial positive change. Fast antennas of the FALMA are not calibrated, so E-change

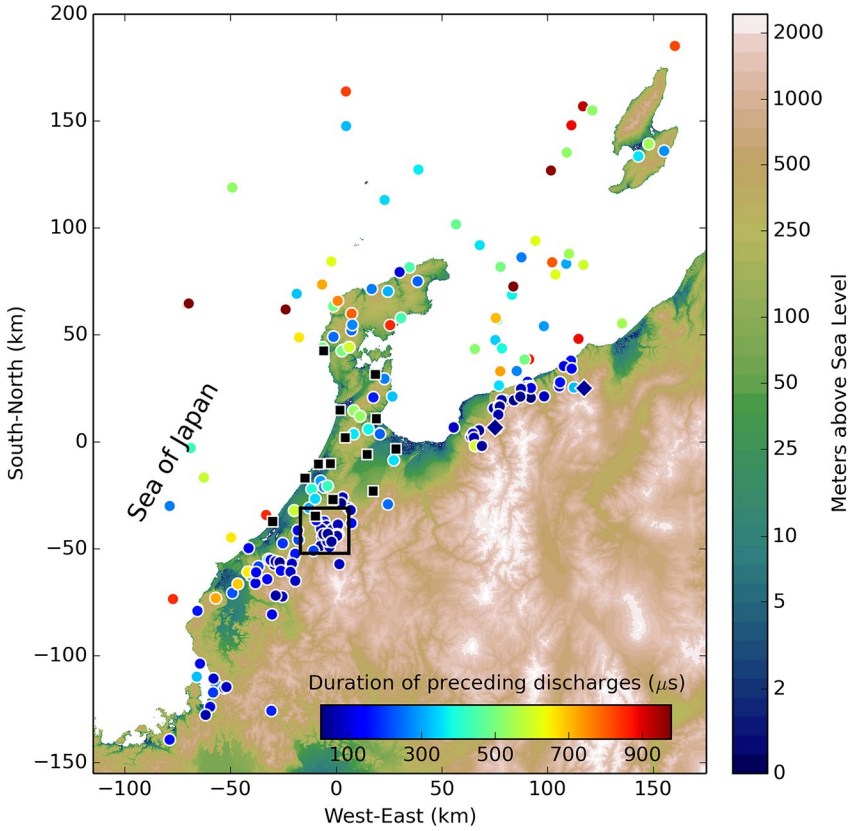

Figure 1. Locations of all strokes with durations of preceding discharges shorter than 1 ms. The color of points indicates the duration of preceding discharges. Black squares represent observation sites of the FALMA. Two blue diamonds represent two positive strokes analyzed in Section 3.4. The area in the black square is further shown in Figure 4. The origin (0, 0) corresponds to the latitude and longitude of (36.76°N, 136.76°E).

magnitudes are expressed in the digital unit (DU). However, peak currents of RSs are estimated by calibrating with the data of the Japanese Lightning Detection Network (JLDN) (e.g., Matsui et al., 2019). Details of the calibration are described in Appendix A.

3. Results

3.1. Strokes With Short (<1 ms) Preceding Discharges

With the simple criteria described in Section 2, 186 events that have the same polarity as negative RSs are identified. We will simply call these events as "strokes" as some of these events have very different E-change waveforms from those of normal negative RSs. Locations of these strokes are shown as colored dots in Figure 1. These strokes produced various types of E-change waveforms. Figures of waveforms of all these strokes are provided in the data repository (see Acknowledgments). Figure 2 shows seven examples of waveforms with different characteristics. In each waveform, the red arrow indicates the first identified pulse in each flash. The first pulse is usually very small and may not be clear in Figure 2. In order to accurately identify the first pulse before each stroke, we always enlarge the waveform to the noise level and carefully compare waveforms recorded by multiple sites to distinguish small signals from noises. Figure S1 shows enlarged waveforms of the first pulses in Figures 2e and 2g. Even so, we admit that it is possible that there are even smaller pulses that could not be identified, especially when the stroke is relatively far away. However, we believe it will not have a significant influence on the results of this study.

Examples in Figure 2 are arranged in order of decreasing duration of preceding discharges (hereafter predischarge duration). The first example in Figure 2a is very similar to a normal RS, except that the predischarge duration is short. Discharges before the stroke clearly show two stages, possibly similar to the PB and

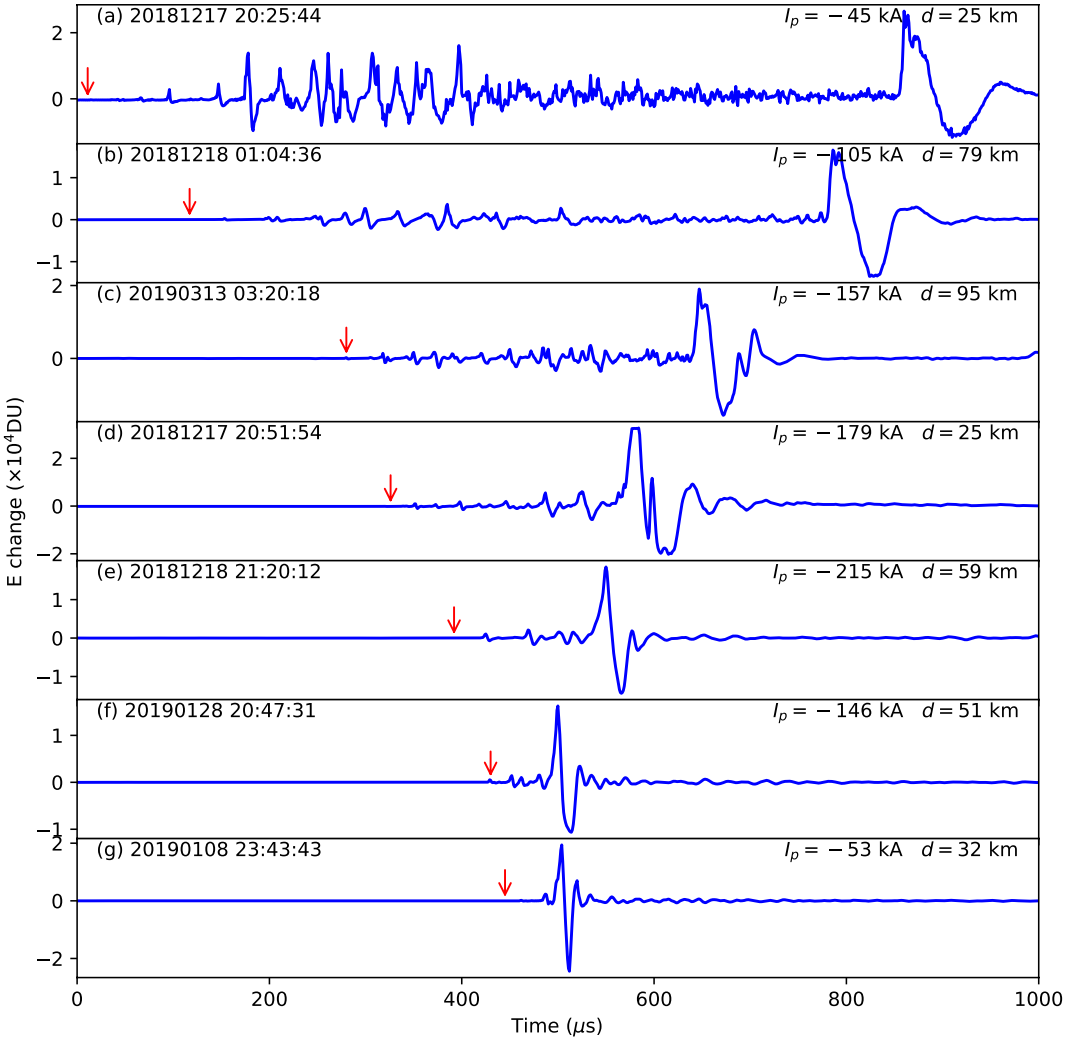

Figure 2. Examples of waveforms of strokes with short (<1 ms) preceding discharges. The value of I_p indicates the stroke peak current estimated using the method described in Appendix A. The value of d indicates the distance between the stroke and the site recording the waveform. The red arrow indicates the first identified pulse. Enlarged waveforms of the first pulses in panels e and g are shown in Figure S1.

stepped leader stages before normal RS, although the PB pulses in this example appear somewhat different from normal PB pulses (Marshall et al., 2013; Nag et al., 2009; Shi et al., 2019b).

The second example in Figure 2b is still similar to a normal RS, and discharges before the stroke may still be divided into two stages, but pulses corresponding to the PB stage are very different from typical PB pulses.

The third example in Figure 2c starts to show clear differences with normal RSs. First, the stroke pulse has similar rise time and fall time, different from a normal RS pulse which usually has much longer fall time than rise time. Second, pulses before the stroke cannot be clearly divided into two stages.

The fourth example in Figure 2d is similar to the third example. The stroke pulse has similar rise time and fall time, and there are no typical PB pulses before the stroke. Note that the waveform is slightly saturated. Also note that this waveform is very similar to those reported by Wada et al. (2020) that were associated with downward terrestrial gamma ray flashes in winter.

The fifth example in Figure 2e starts to resemble LBE pulses reported by Wu et al. (2014). The stroke pulse is a simple bipolar pulse and there are only a few small pulses before.

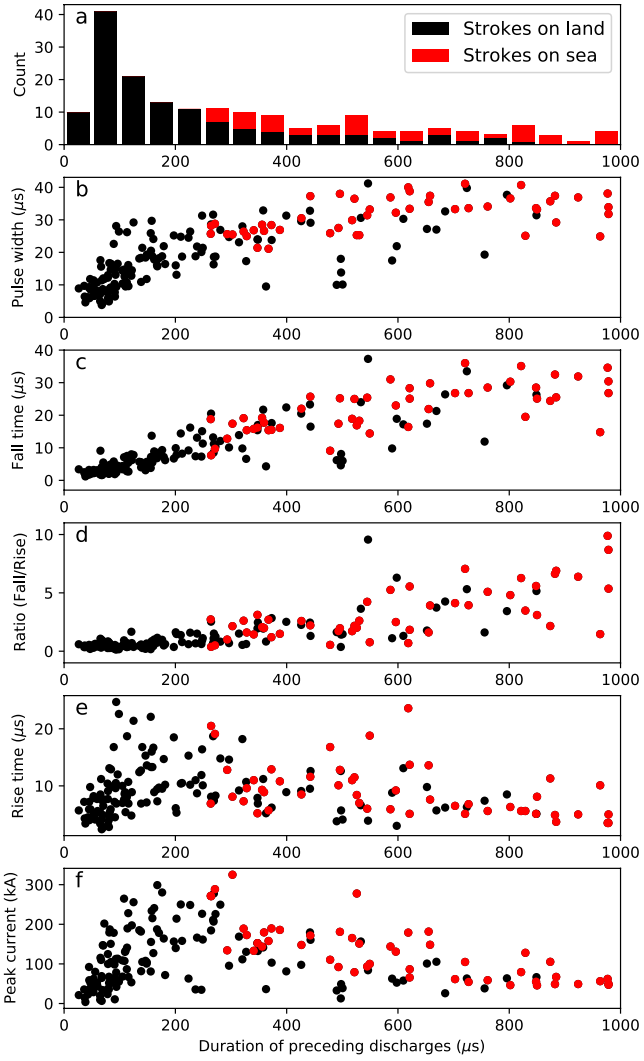

Figure 3. (a) Distribution of the preceding discharge duration and its relationship with (b) the pulse width (c) the fall time (d) the ratio of the fall time to the rise time (e) the rise time and (f) the estimated peak current (absolute value) of the stroke pulse. Black points represent strokes located on land and red ones on the sea.

Examples in Figures 2f and 2g are also LBE-like pulses with the duration of preceding pulses shorter than 100 μs.

If we directly compare Figures 2a and 2g, it is clear that these two waveforms are distinctly different, and the pulse in Figure 2g is apparently different from a normal RS pulse. However, from Figures 2a–2g, these waveforms actually change gradually; any two neighboring waveforms share certain similarities. This is also evidence that these different waveforms are all produced by RS-like processes but under different conditions. We can also see that most of the strokes in Figure 2 have very large peak currents. As reported by Wu et al. (2020b), upward negative leaders from tall grounded objects in winter are often initiated by such strokes.

3.2. Characterizing Compact Strokes

From Figure 2, it appears that as the predischarge duration decreases, characteristics of the stroke pulse also gradually change. For example, from Figures 2a–2g, it seems the pulse width decreases and the rise time relative to the fall time increases. In order to systematically investigate the relationship between the predischarge duration and characteristics of the stroke pulse, Figure 3 shows the distribution of the predischarge duration and its relationship with various parameters of the stroke pulse with red points representing strokes located on the sea and black ones on land. Definitions of the rise time, fall time, and pulse width are illustrated in Figure S2. Note that 6 strokes which saturated all sites and thus waveform parameters cannot be accurately calculated are not included here.

From Figures 3b–3e, we can see that strokes with predischarge durations shorter and longer than about 200 μs show different characteristics on the relationship between the predischarge duration and various parameters. First, Figure 3b shows an overall positive correlation between the predischarge duration and the pulse width of the stroke pulse. However, for strokes with predischarge durations shorter than 200 μs, an approximately linear positive correlation exists, while for strokes with longer predischarge duration, the positive correlation gradually decreases, and when the duration is longer than about 600 μs, the stroke pulse width is generally stable, almost unrelated with the duration. Similar correlation can also be found between the predischarge duration and the fall time of the stroke pulse as shown in Figure 3c. Further, the ratio of the fall time to the rise time of the stroke pulse is calculated, and its relationship with the predischarge duration is shown in Figure 3d. As the predischarge duration increases, the ratio shows an overall increasing trend. However, for strokes with the predischarge duration shorter than about 200 μs, the ratio has little variation, distinctly different from strokes with longer predischarge duration.

More interestingly, Figure 3e shows the relationship between the predischarge duration and the rise time of the stroke pulse. For strokes with predischarge durations shorter than about 200 μs, a clear positive correlation exists, while for strokes with predischarge durations longer than about 200 μs, a clear negative correlation exists. Similarly, Figure 3f shows the relationship between the predischarge duration and the estimated stroke peak current (absolute value), and clear positive and negative correlations can be seen, respectively, for strokes with predischarge durations shorter and longer than about 200 μs.

From the above results, it is clear that strokes with predischarge durations shorter and longer than about 200 μs have systematically different characteristics. It is also clear that strokes with long predischarge durations are similar to normal RSs. It is well understood that the peak current of the first RS in a negative CG flash is negatively correlated with the duration of preceding discharges including PB and stepped leader

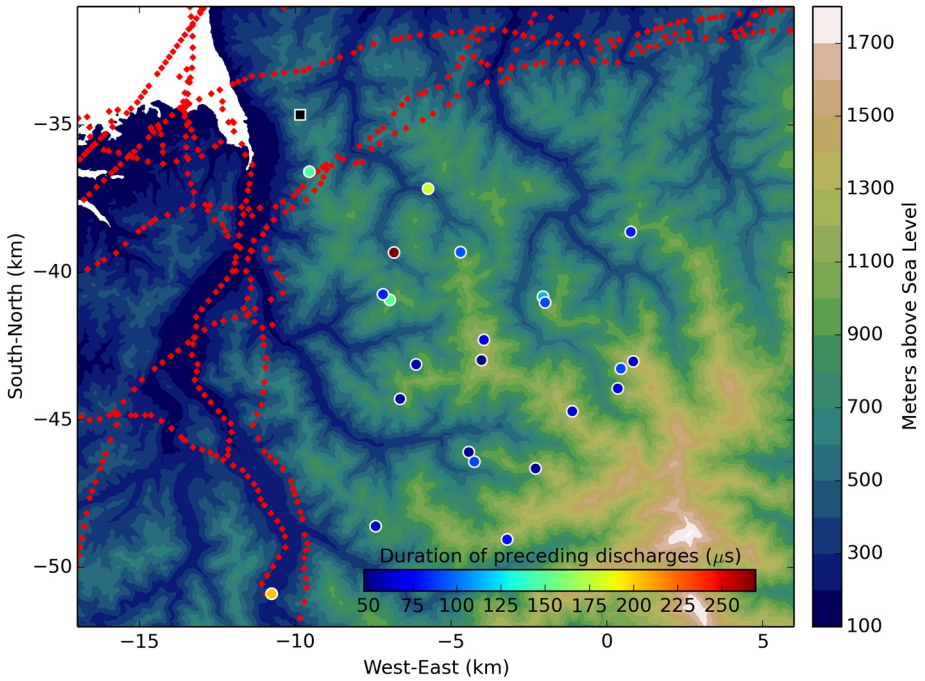

Figure 4. Strokes in a mountain area (the black square in Figure 1). Small red diamonds represent power transmission towers.

(Nag & Cummins, 2017; Shi et al., 2019a; Zhu et al., 2015), similar to the result in Figure 3f for strokes with predischarge durations longer than about 200 μs. It is also well known that the fall time of RS pulses is usually much larger than the rise time (e.g., Lin et al., 1979), similar to the result in Figure 3d for strokes with large predischarge durations. Moreover, the pulse width and fall time of RS E-change waveforms are not known to be correlated with the predischarge duration, in agreement with the result in Figures 3b and 3c for strokes with long predischarge durations. Therefore, we conclude that strokes with long predischarge durations are essentially the same as normal RSs.

On the other hand, strokes with short predischarge durations (roughly <200 μs) are apparently different from normal RSs. According to Figure 1, strokes with short predischarge durations (dark blue dots) all occurred on land. In fact, they are not just on land but are also relatively far away from the coast. This indicates that these strokes may be associated with the high elevation in mountain areas, which can also explain the extremely short predischarge duration. In order to verify this speculation, Figure 4 shows locations of strokes in the black square in Figure 1, which seems to be a hot spot of strokes with short predischarge durations. From Figure 4, we can see that most strokes occurred at locations with an elevation of about 1 km. Interestingly, most strokes seem to occur on mountains but not in valleys between mountains. Figure 4 also shows locations of power transmission towers with red dots identified from Google Earth. It is clear that most strokes are not associated with transmission towers. In fact, in the area where most strokes occurred in Figure 4, no human-made tall objects can be identified. Therefore, strokes with short predischarge durations are mostly associated with high mountains but not tall objects such as transmission towers.

It should be noted that although no strokes were detected in regions with even higher elevations, this is simply because winter thunderstorms usually cannot move over the mountain area. Figure 5 shows the density map of all located lightning discharge sources during the winter observation. We can see that lightning discharges mainly clustered along the coastline and rarely occurred more than about 50 km inland.

Figure 6 further shows the relationship between predischarge durations and elevations of stroke locations with red points representing strokes within 50 km from the center of the FALMA network (the origin in Figure 1) and blue points more than 50 km away from the center. It demonstrates that strokes with shorter predischarge durations are more likely to occur at locations with higher elevations. Particularly, red points

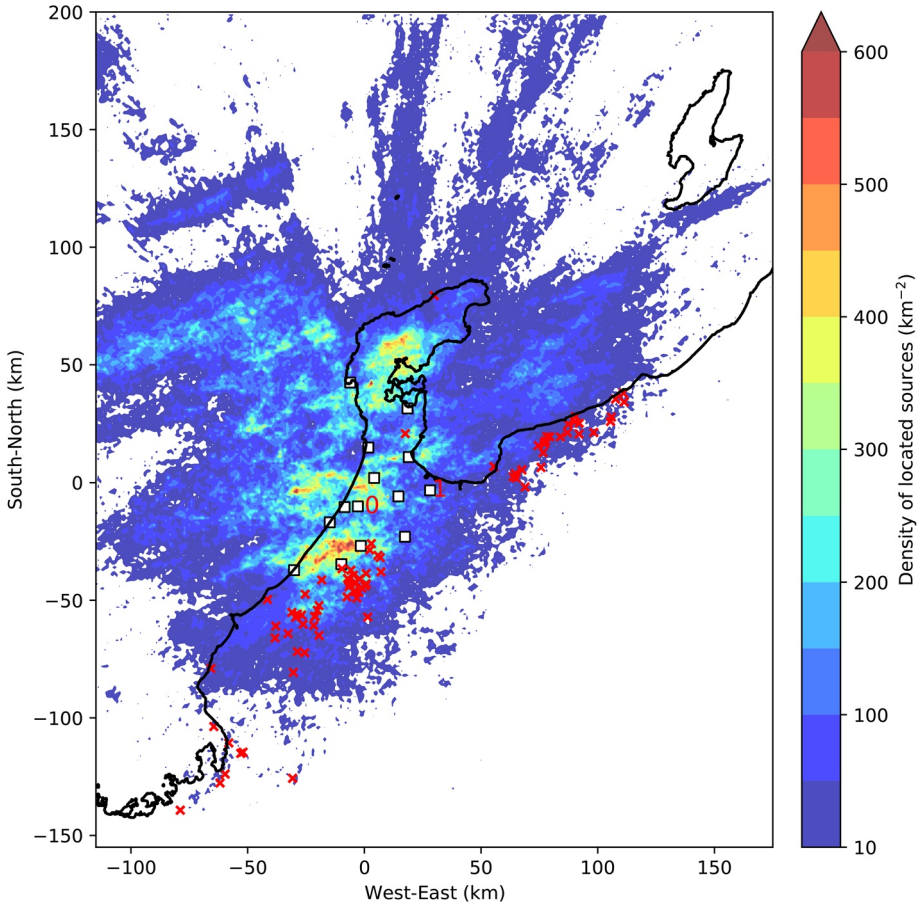

Figure 5. Density (per square km) of all located lightning discharge sources during the winter observation. White squares represent observation sites of the FALMA. Red crosses represent strokes with durations of preceding discharges shorter than 200 μs. Numbers 0 and 1 indicate two sites used in Appendix A.

with predischarge durations shorter than 200 μs mostly occurred at locations with elevations higher than 400 m. Some blue points with short predischarge durations occurred at locations with low elevations, but they may be due to uncertainties in location results as these strokes are relatively far away from the FALMA network. Still, even for blue points, most of them occurred at locations with elevations higher than 200 m. On the other hand, strokes with long predischarge durations, for example, larger than 400 μs, mostly occurred at locations with elevations lower than 200 m. This result fully demonstrates the association between strokes with extremely short predischarge durations and high-elevation areas such as mountains.

Based on the above analysis, we conclude that the extremely short (roughly <200 μs) preceding discharges are mainly due to the extremely short distances between high mountain tops and low negative charge regions in winter thunderstorms. This result also indicates that these strokes have extremely short channels, which will be estimated in Section 3.3. We also demonstrated that these strokes are systematically different from normal RSs. Therefore, in order to distinguish these special strokes from normal RSs, we will call them "compact RSs." It is clear that characteristics of compact RSs are closely related with durations of preceding discharges. For simplicity, compact RSs along with preceding discharges will be referred to as "compact strokes." In the remaining part of this study, we will focus on strokes with predischarge durations shorter than 200 μs that are most likely compact strokes.

3.3. Channel Length Estimation of Compact Strokes

As explained in Section 2, the accuracy of height results is low for winter lightning mainly because winter lightning usually has low source altitudes. It is well understood that for a lightning mapping system

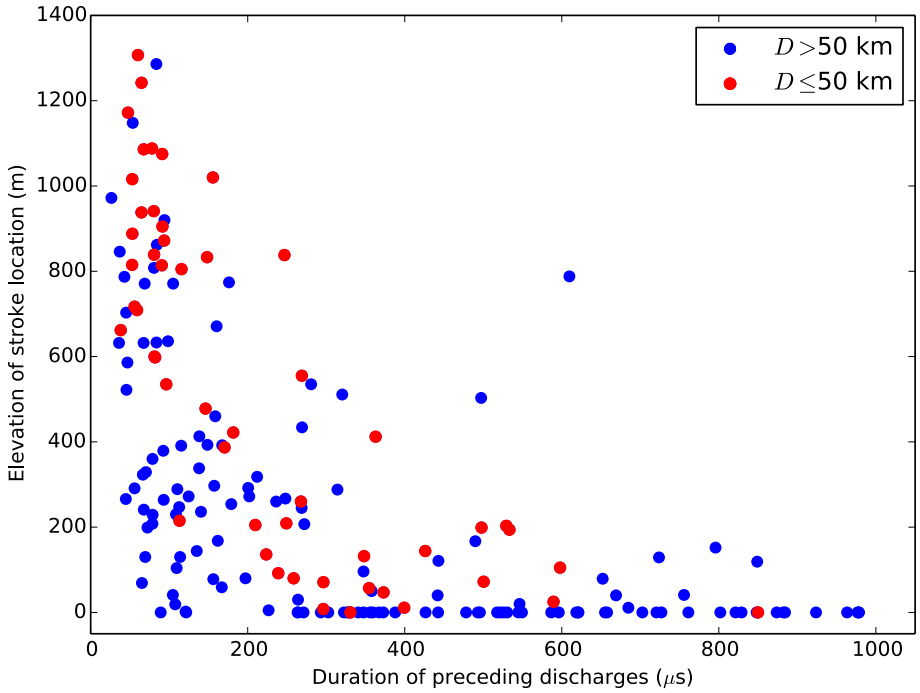

Figure 6. Scatterplot of the elevation of stroke locations versus the duration of preceding discharges. Red points represent strokes located within 50 km from the center of the FALMA (the origin in Figure 1) and blue ones represent those beyond 50 km.

consisting of observation sites at similar altitudes, the uncertainty in height results for discharges near the ground is very large (Bitzer et al., 2013; Thomas et al., 2004; Yoshida et al., 2014). Considering the possibility that compact strokes occur near the ground and have extremely short channels, it is highly unreliable to use the location results to calculate channel lengths.

The fact that the vast majority of compact strokes are negative polarity (lowering negative charges) indicates that they likely initiate from the lower edge of the main negative charge region of a normal dipole or tripole structure. It is well known that the main negative charge region is usually found in the temperature range of $-20 \sim -10$°C (e.g., Stolzenburg & Marshall, 2008; Williams, 1989), and negative CG flashes are usually found to initiate in the temperature range of $0 \sim -10$°C (Mecikalski & Carey, 2017; Wu et al., 2015), corresponding to the lower edge of the main negative charge region. Therefore, we first look at the relationship between isotherms of 0°C and −10°C and elevations of stroke locations. Compact strokes (predischarge durations <200 μs) located within 50 km from the center of the FALMA are selected, and elevations of their locations and isotherms of 0°C and −10°C at the corresponding time are shown in Figure 7a. The isotherm data are provided by the Japan Meteorological Agency, measured at 9:00 and 21:00 local time every day at a location about 80 km away from the center of FALMA. We can see that elevations of stroke locations are generally at or slightly higher than the isotherm of 0°C and are always lower than the isotherm of −10°C. Interestingly, if we calculate differences between isotherms of 0°C and −10°C and elevations of stroke locations, they show weak correlations with the predischarge duration as shown in Figures 7b and 7c. Pearson correlation coefficients for both Figures 7b and 7c are 0.35. The correlation between the altitude difference and the predischarge duration can be interpreted as follows: the flash initiates at the altitude of a certain temperature with a negative leader going directly down to the ground, so the predischarge duration is the propagation time of the leader. The weak correlation is actually rather significant considering various uncertainties in the data. For example, the temperature profile is measured only twice a day and may be somewhat different from that at the time of the lightning; the negative charge region may not always be at the same temperature; the downward negative leader may not always propagate with the same velocity. Moreover, there are several clear outliers in Figures 7b and 7c which significantly decrease correlation

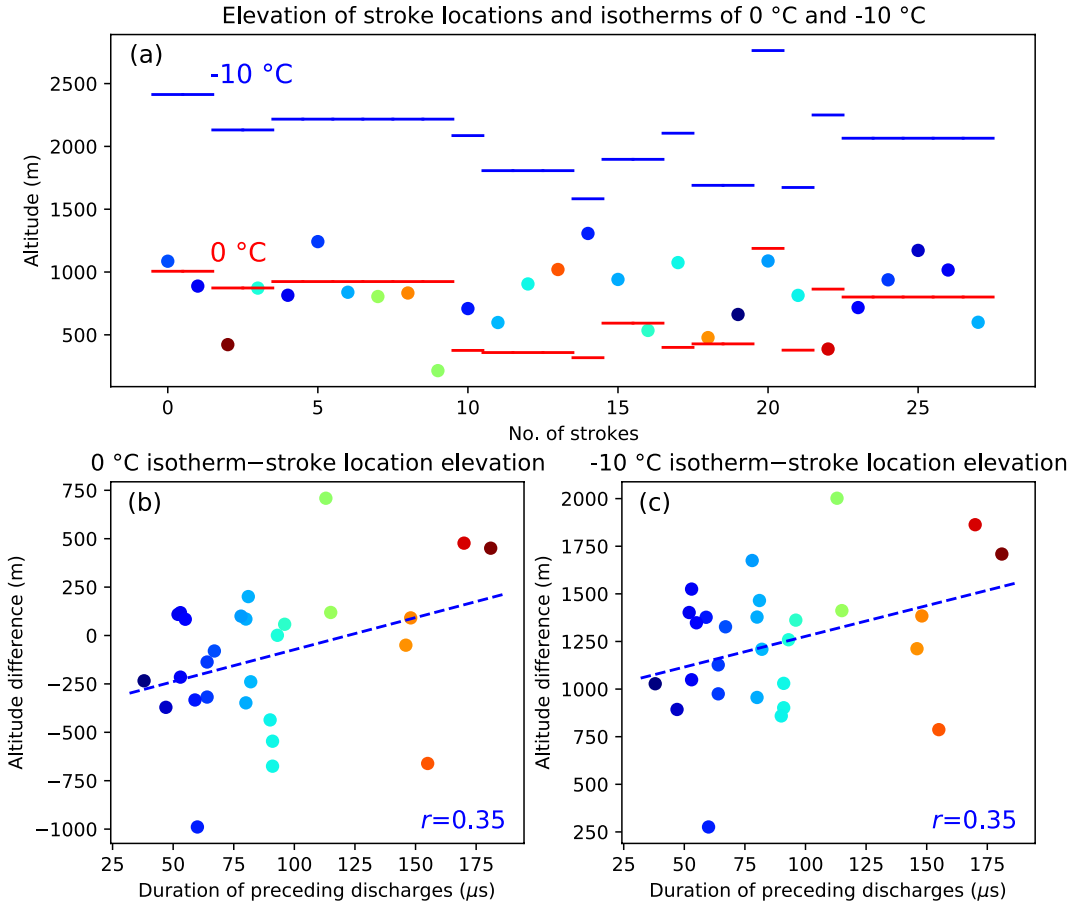

Figure 7. (a) Elevation of stroke locations and corresponding isotherms of 0°C (red lines) and −10°C (blue lines). Scatterplots of the altitude difference between (b) 0°C isotherm/(c) −10°C isotherm and stroke location elevations versus durations of preceding discharges. Blue dashed lines are linear regression lines and the value of *r* represents the correlation coefficient. The color of points indicates the duration of preceding discharges.

coefficients. For example, if we exclude the point at the bottom right in Figures 7b and 7c, correlation coefficients increase to 0.49 and 0.47.

Based on the above analysis, we can roughly estimate the overall velocity of downward negative leaders preceding compact RSs as slopes of the regression lines in Figures 7b and 7c, and the stroke channel length can be estimated from the velocity and the predischarge duration. Slopes of the regression lines (blue dashes lines) in Figures 7b and 7c are 3.31 and 3.22 m/μs (10^6 m/s), respectively. The average of the two values, 3.27×10^6 m/s is treated as the overall velocity of the downward negative leader. Assuming negative leaders preceding compact RSs all had this velocity, channel lengths of compact strokes can be calculated by multiplying the velocity by the predischarge duration. The distribution of estimated channel lengths of compact strokes in Figure 7 is shown in Figure 8a. Further, the initiation altitude can be estimated by adding the elevation of the stroke location and the channel length. The distribution of the estimated initiation altitudes are shown in Figure 8b. The distribution of corresponding temperatures at initiation altitudes are shown in Figure 8c.

The velocity of 3.27×10^6 m/s is about one order of magnitude larger than velocities of negative leaders in the PB stage of negative CG flashes observed during the summer observation by the FALMA (Shi et al., 2019a). However, it is also a reasonable result considering the low initiation altitudes. Wu et al. (2015) demonstrated that velocities of initial negative leaders during the PB stage in intracloud lightning flashes increased with decreasing initiation altitudes; leaders initiating at 10 km had velocities around 10^5 m/s while those

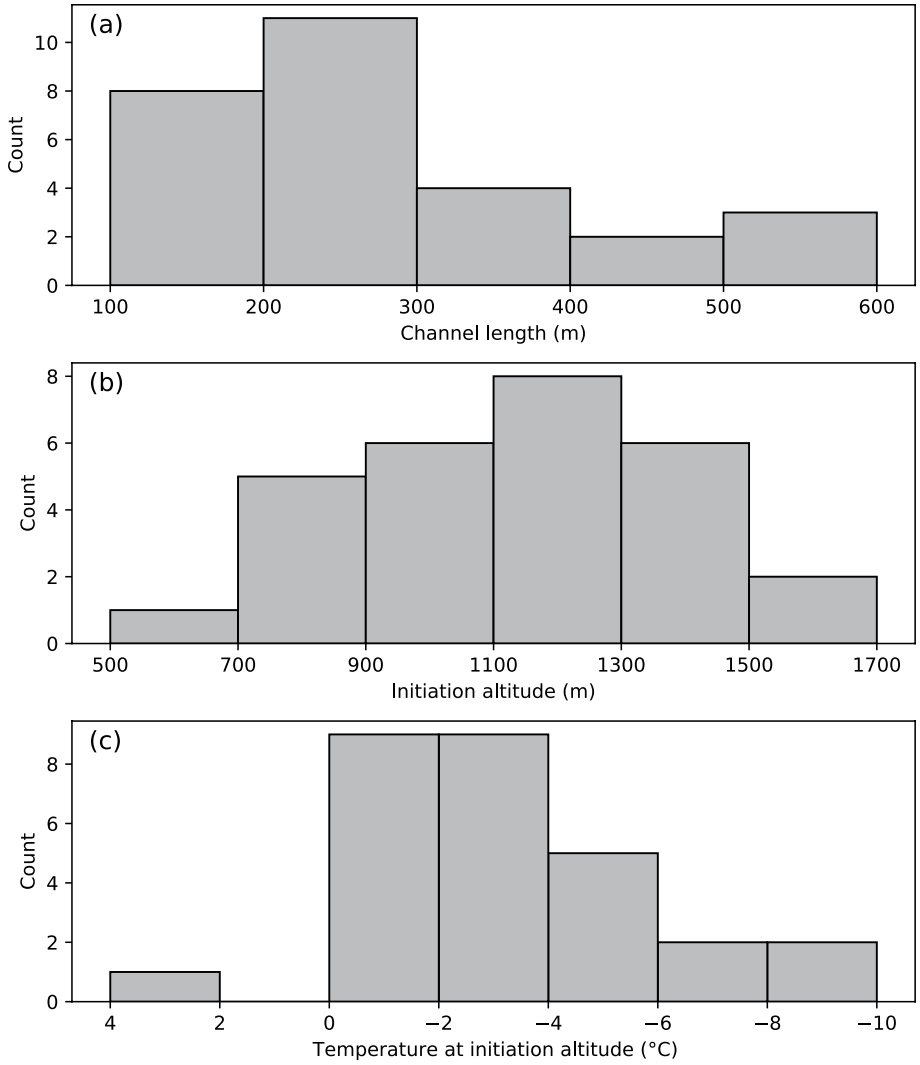

Figure 8. Distributions of (a) estimated channel lengths of compact strokes, (b) initiation altitudes of compact strokes, and (c) temperatures at initiation altitudes.

initiating at 5 km had velocities around 10^6 m/s. It is likely that a similar relationship also exists in negative CG flashes. Therefore, the velocity of 3.27×10^6 m/s is a reasonable value for leaders initiating below 2 km.

Estimated channel lengths of compact strokes range from 124 to 592 m with an arithmetic mean of 292 m. Channel lengths of normal RSs in summer thunderstorms can be inferred from their initiation altitudes, which are generally 5~6 km (Shi et al., 2019a; Wu et al., 2015). Therefore, channel lengths of compact strokes are at least one order of magnitude shorter than those of normal RSs.

Initiation altitudes of compact strokes are estimated to range from 585 to 1,527 m with an arithmetic mean of 1,113 m. The corresponding temperatures are mainly in the range of $0 \sim -10$°C, in agreement with the concept that negative CG flashes initiate from the lower edge of the main negative charge region and observations of temperatures at lightning initiation altitudes (Mecikalski & Carey, 2017; Wu et al., 2015).

3.4. Possible Existence of Positive Compact Strokes

E-change waveforms of two possible positive compact strokes are shown in Figure 9. Their locations are shown as blue diamonds in Figure 1. Elevations of the stroke locations are 451 and 485 m, respectively, for strokes in Figures 9a and 9b. They were produced about 40 min apart with a distance of 46 km. These two

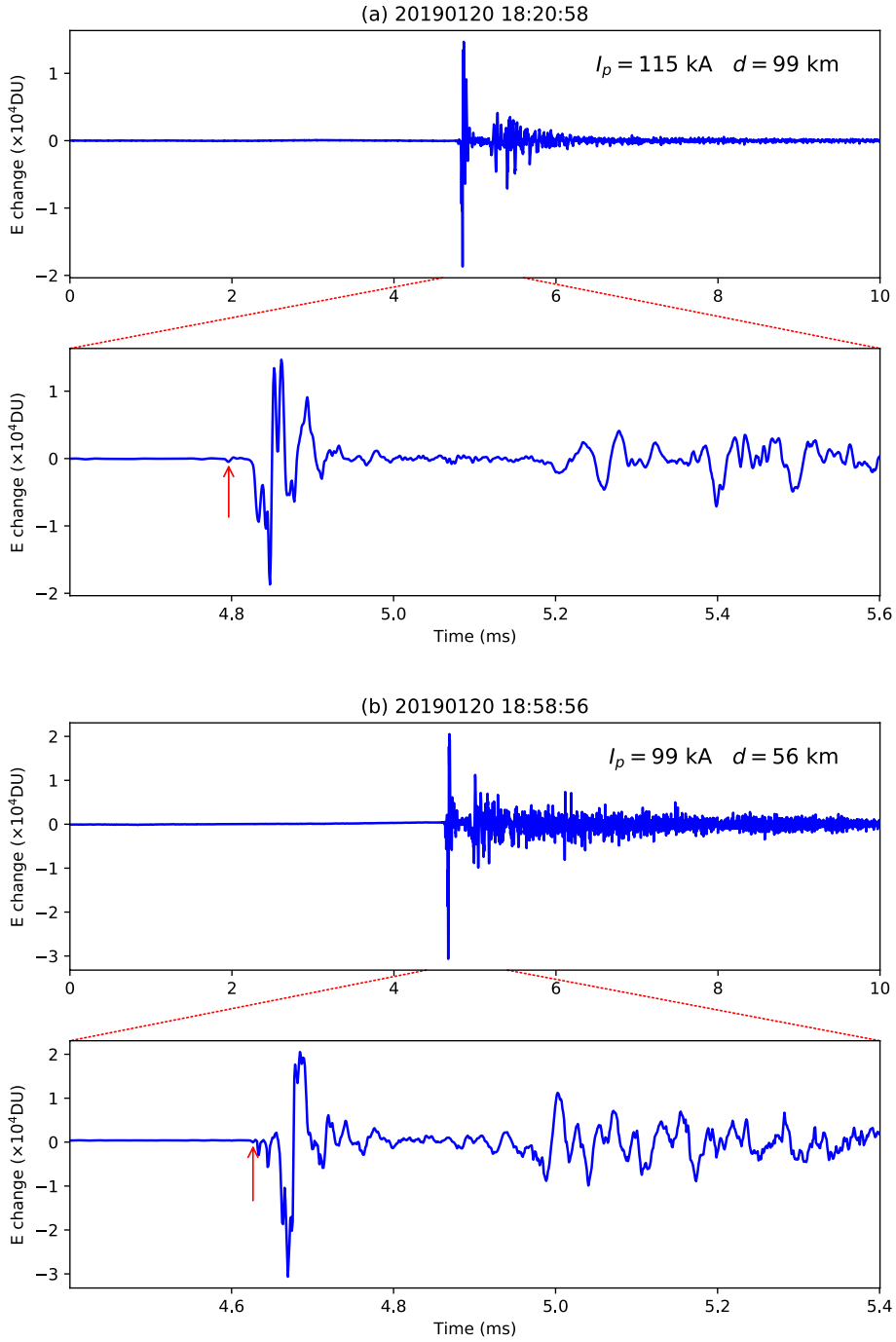

Figure 9. Waveforms of two possible compact strokes having the same polarity as positive RSs. The value of I_p indicates the estimated stroke peak current. The value of d indicates the distance between the stroke and the site recording the waveform. The red arrow indicates the first identified pulse.

strokes have estimated peak currents of 115 and 99 kA. For each stroke, there were only a few small pulses right before the stroke pulse. The time difference between the first identified pulse (red arrow in Figure 9) and the peak of the stroke pulse was only about 50 μs.

A clear difference with negative compact strokes is that the two positive strokes in Figure 9 are both followed closely by some irregular pulses while negative compact strokes are not as shown by the examples in Figure 2. These irregular pulses may be produced by the RS wave, which carries negative charges, when it

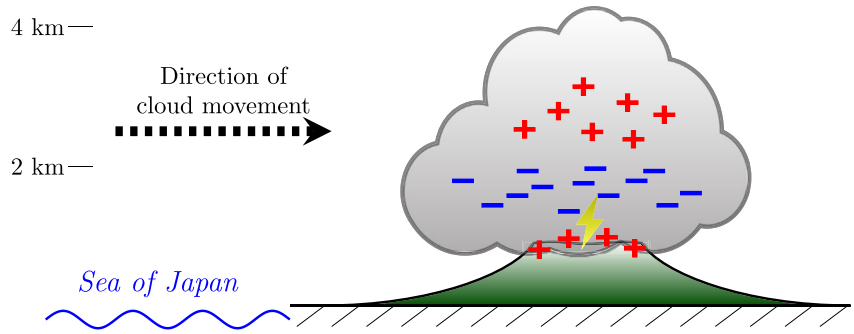

Figure 10. Illustration of the usual condition for the production of compact strokes. The thunderstorm is assumed to carry a normal tripole charge structure, and the lower positive charge region is at a comparable altitude to the mountain surface.

creates new in-cloud channels soon after traveling through the short stroke channel. In the case of negative strokes, the RS wave carries positive charges, so even if it continues propagating in the cloud, it is usually very quiet and may not produce detectable pulses in the LF band.

With the small number of events, we are not able to determine whether they are systematically different from normal positive RSs and can be considered as positive compact strokes. However, one clear conclusion is that such special positive strokes are very rare. It is well known that winter thunderstorms produce frequent positive CG flashes (Goto & Narita, 1995; Miyake et al., 1992). As reported by Wu et al. (2020a), during the same winter observation as that in this study, 263 positive CG flashes were observed, and these only include flashes near the FALMA network. One possible reason for the rarity of positive compact strokes is that positive CG flashes in winter usually initiate from the upper edge of the positive charge region in an inverted dipole or tripole structure as reported by Wang et al. (2021); positive leaders initiating positive RSs usually originate from in-cloud negative leaders, and consequently, there are usually considerable discharges before positive RSs. Another possible reason is that even if a positive stroke similar to the negative compact stroke occurs, the downward positive leader initiating the positive RS may be much slower than the negative leader initiating negative compact RSs, and the time difference between the start of the flash and the first stroke is longer than 1 ms so such cases were not identified with the criteria described in Section 2.

4. Discussion

4.1. Conditions for the Production of Compact Strokes

From the above analysis, it is clear that the most important characteristic of compact strokes is the short channel, which is estimated to be shorter than 600 m and on average only about 300 m. Compact strokes are mainly produced in small gaps between mountain tops and the main negative charge region in thunderclouds as illustrated in Figure 10. According to Figure 6, it seems that negative strokes occurring at locations with elevations higher than 600 m are almost always compact strokes. Moreover, at locations with elevations from 200 to 600 m, most strokes have predischarge durations shorter than 200 μs. Although most of these strokes are relatively far away from the FALMA network and may have low location accuracy, it seems likely that an elevation of above 200 m already has a significant effect in increasing the chance of the occurrence of compact strokes. By comparison, if we look at strokes with predischarge durations longer than 400 μs in Figure 6, we can see almost all of them occurred at locations with elevations lower than 200 m.

As illustrated in Figure 10, winter thunderstorms in Japan develop from the sea and move toward the land. Soon after the landing, they encounter mountain areas (see Figure 1) and dissipate, and they rarely move over the mountain area. We can also look at the density map of lightning discharge sources in Figure 5, and we can see that most lightning discharges in winter occur on the sea and along the coastline. Figure 5 also shows the locations of strokes with predischarge durations shorter than 200 μs, which are inferred to be most likely compact strokes, with red cross signs. We can see that most compact strokes occurred outside the high density area and at the inland side. This indicates that compact strokes usually occur during the dissipating stage of winter thunderstorms when the storms start to climb the mountains. It is possible that

when the storm is dissipating, some negative charges may fall down to lower altitudes. Therefore, even at relatively low elevations of 200–600 m, most strokes are compact strokes.

In Figure 6, there are also some strokes occurring at locations with elevations lower than 200 m and having predischarge durations shorter than 200 μs. We checked the locations of these strokes and found some of them were located near tall grounded objects such as power transmission towers and windmills. This may not be a coincidence; in fact, in Figure 4, there are also two strokes located very near transmission towers. Although we concluded in Section 3.2 that most compact strokes are not associated with tall grounded objects, it is possible that the existence of tall grounded objects can increase the chance of the occurrence of compact strokes in low-elevation areas. This is because that when a downward negative leader approaches a tall grounded object, it may initiate a relatively long upward connecting leader, and the attachment point can be higher than normal, resulting in a condition similar to the existence of a mountain.

4.2. Reasons for the Differences Between Compact and Normal Return Strokes

The most significant difference between compact RSs and normal RSs is that peak amplitudes of compact RSs increase with increasing predischarge durations while those of normal RSs decrease with increasing predischarge durations as demonstrated in Figure 3f. In order to explain this difference, we first need to clarify the reason for the negative correlation between predischarge durations and stroke peak amplitudes for normal RSs. The negative correlation for normal RSs has also been reported by previous studies (Nag & Cummins, 2017; Shi et al., 2019a; Zhu et al., 2015). The reason is that both the velocity of stepped leaders initiating RSs and the peak amplitude of RSs are positively correlated with the ambient electric field strength, and because the predischarge duration is negatively correlated with the velocity of stepped leaders, the duration is also negatively correlated with the peak amplitude of RSs. Shi et al. (2019a) also showed that the peak amplitude of RSs has no correlation with the initiation altitude, so the negative correlation between the predischarge duration and the peak amplitude for normal RSs is generally a manifestation of the positive correlation between the stepped leader velocity and the peak amplitude.

Next, we will demonstrate that discharges preceding compact RSs correspond to the PB stage and there are no preceding stepped leaders and thus the correlation described above for normal RSs does not exist. According to Figure 7a, elevations of stroke locations are generally comparable to or slightly higher than 0°C isotherm. Assuming thunderstorms carry the normal tripole charge structure, it is likely that mountain surfaces where compact strokes occur are at comparable altitudes to the lower positive charge region. Therefore, when winter thunderstorms move to the mountain area, some positive charges may move to the mountain surface and some may just be stopped at the mountain slope. Considering the effect of the main negative charge region, the mountain surface and the near-surface space carry positive charges and are virtually the lower positive charge region of the tripole structure. As a result, leaders initiating compact RSs are confined in the so-called "enhanced field region" (Shi et al., 2019a) between the main negative charge region and the lower positive charge region and correspond to the PB stage in normal negative CG flashes as illustrated in Figure 10.

Shi et al. (2019a) also showed that leader velocities during the PB stage have a much weaker correlation with the peak amplitude of RSs than velocities of stepped leaders do. As a result, relationships responsible for the negative correlation between predischarge durations and peak amplitudes for normal RSs only have weak effects for compact strokes. Another factor, the stroke channel length, may have a larger influence on the peak amplitude of compact RSs. Figure 11 shows correlations between altitude differences (0°C, −10°C isotherms and elevations of stroke locations) and peak currents of compact RSs. The same compact strokes as those in Figure 7 are analyzed here but the correlations are slightly stronger than those in Figures 7b and 7c. These correlations may indicate a relationship between the stroke channel length and the peak current of compact RSs. With increasing channel length, more charges will be induced at both ends of the channel, which may be responsible for stronger strokes.

Considering that discharges preceding compact RSs correspond to the PB stage, we can also explain the positive correlations between the pulse width and the predischarge duration (Figure 3b) and between the fall time and the predischarge duration (Figure 3c). Both the pulse width and the fall time of the stroke pulse are a manifestation of the time for the RS wave to neutralize charges deposited by preceding leaders in the

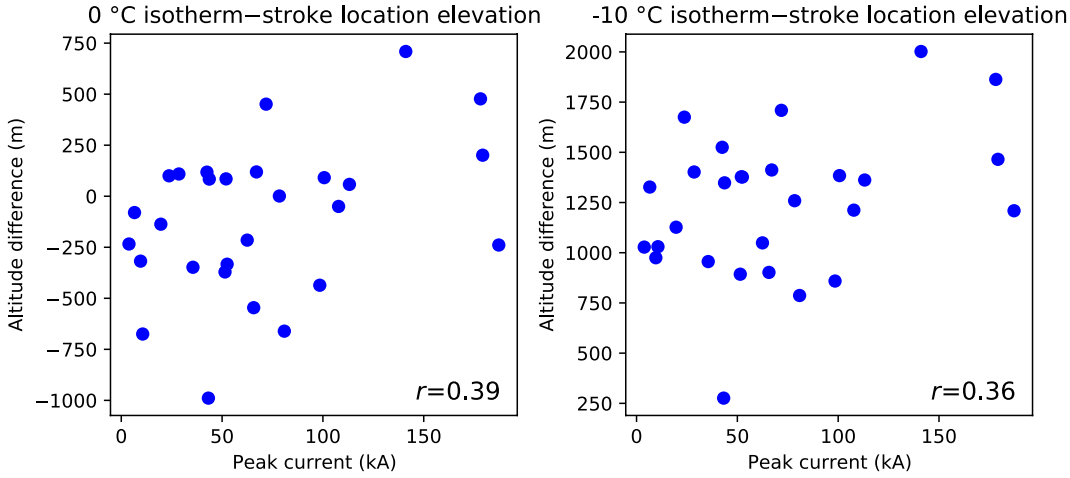

Figure 11. Scatterplot of the altitude difference between (a) 0°C isotherm and (b) −10°C isotherm and stroke location elevations versus peak currents of compact return strokes. The value of *r* represents the correlation coefficient.

channel. During the PB stage, it is likely that the leader has not yet developed branches, so the longer the channel, the more the time needed to neutralize charges in the channel. However, for normal negative CG flashes, the stepped leader is the major leader process before the first RS. A negative stepped leader normally creates abundant branches and the stroke wave will need to neutralize charges in all of the branches. As a result, the time needed is largely dependent on branch characteristics such as branch numbers and lengths, and therefore the positive correlations do not exist for normal RSs.

Based on the above analysis, it is possible that being confined in the region between the main negative and the lower positive charge regions is a fundamental characteristic of compact strokes. In other words, as long as the initiation point of the RS (the connection point of the downward negative leader and the upward connecting leader) is in or above the lower positive charge region, the resulting RS has the characteristics of compact RSs. If this speculation is true, we can also explain why some compact strokes seem to be associated with tall grounded objects (Section 4.1). If an initial negative leader propagates downward to a location with no tall objects (normal situation), it just results in a normal RS. However, occasionally the initial leader propagates downward to a location near a tall object, then it may initiate a long upward positive leader; the connection point may be higher than the lower positive charge region and a compact RS is produced.

4.3. Comparison With Negative Return Strokes in Upward Lightning

Although in Section 4.1 we described the possibility that some compact strokes occurring at low-elevation areas are associated with tall grounded objects, we want to emphasize that compact strokes are fundamentally different from upward lightning flashes. Upward lightning flashes are defined as lightning flashes initiated by an upward leader from a grounded object, but compact strokes apparently start with in-cloud leader processes.

In winter thunderstorms, upward lightning flashes starting with an upward positive leader from tall grounded objects and followed by negative RSs in the same channel as the upward leader are commonly observed. However, they produce distinctive E-change waveforms and can be easily identified, and they are different from waveforms produced by compact strokes. One example of the waveform produced by a self-initiated upward negative flash including four RSs is shown in Figure 12. The following characteristics indicate that these waveforms are produced by a self-initiated upward lightning flash. First, before the first RS, no pulses can be recognized as shown in Figure 12b. This is because the upward negative flash starts with an upward positive leader which is usually quite weak and is basically invisible to a remote LF antenna. Second, all four RSs produce similar waveforms and pulse widths are all very narrow (~10 μs). Third, all four RSs produce pulses with much larger positive peaks than negative peaks, different from pulses produced by compact RSs which usually have comparable positive and negative peaks. Finally, we confirmed from Google Earth that

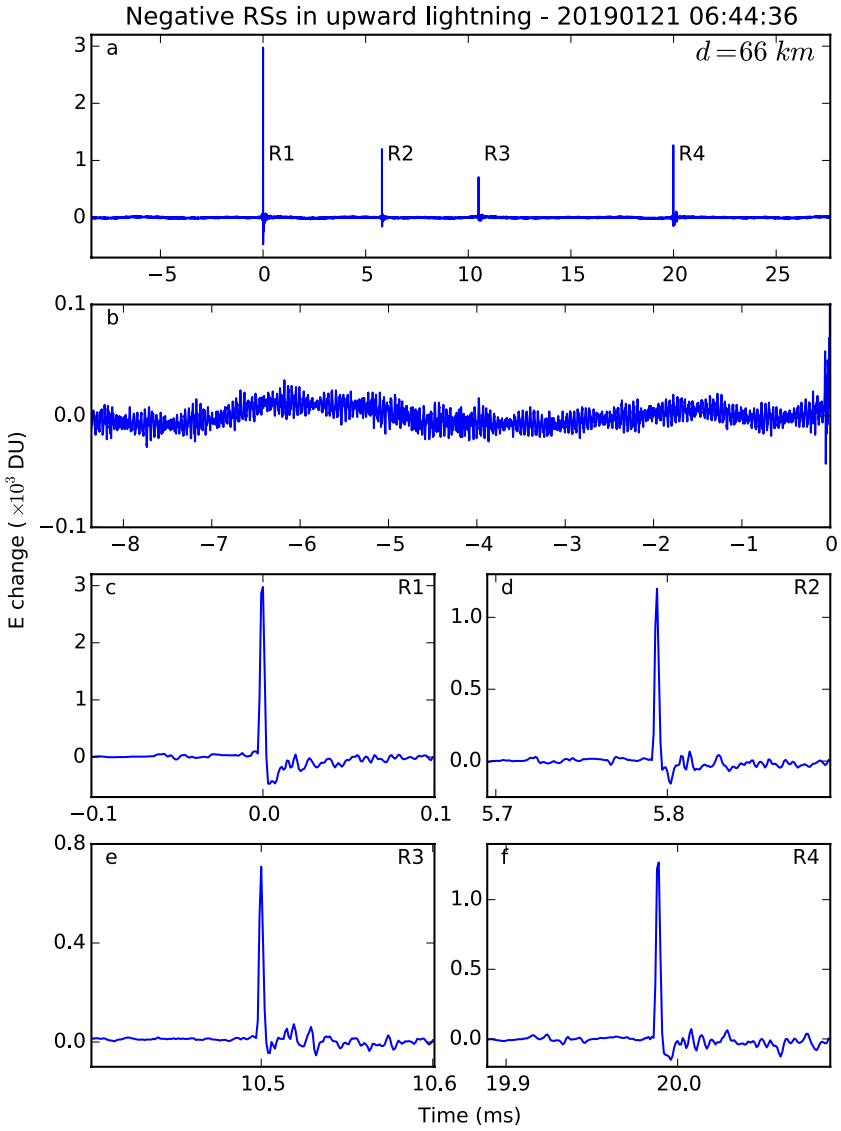

Figure 12. Waveforms produced by a self-initiated upward lightning flash containing four negative return strokes (RSs). R1 ~ R4 indicates four RSs. Panel (b) shows the enlarged waveform right before the first RS. (c) ~ (f) show waveforms of the four RSs on a time scale of 200 μs.

all four RSs are located near a tall object, in this case, a windmill. Zhu et al. (2017) also reported similar waveforms produced by negative RSs in an upward lightning flash striking a tower.

Apart from different waveforms from upward lightning flashes, many results in this paper indicate that compact strokes are not upward lightning. The most definitive evidence is that compact strokes always start with characteristic pulses having the same polarity as negative RSs. According to their polarity, these pulses can be produced by upward positive leaders or downward negative leaders. In the case of negative upward lightning flashes, they start with upward positive leaders and may be followed by negative downward dart leaders, both of which are usually quiet in the LF band, as shown by the example in Figure 12. The fact that compact strokes always start with such characteristic pulses indicate that these pulses are produced by downward negative leaders in the virgin air, that is, initial negative leaders in the PB stage. Therefore, compact strokes start with the PB stage just like normal negative CG flashes.

Ishii and Saito (2009) reported characteristic E-change waveforms produced by strong winter lightning associated with power transmission-line faults. Those waveforms are similar to waveforms of compact

strokes, and they were interpreted as being produced by upward lightning based on the fact that they were coincident with transmission-line faults and the assumption that most lightning flashes striking transmission towers in winter are upward lightning. However, the analysis by Ishii and Saito (2009) was based on the data of lightning discharges associated with transmission-line faults, so naturally these discharges are coincident with transmission-line faults and this fact does not say anything about whether they are upward lightning. Moreover, the number of negative discharges associated with transmission-line faults during a 10-year period analyzed by Ishii and Saito (2009) was only 21, so it is likely that the discharges analyzed by Ishii and Saito (2009) are a subset of compact strokes that struck tall grounded objects such as those mentioned in Section 4.1.

Therefore, we conclude that the compact stroke is not a type of upward lightning; instead, it is a discharge process similar to the PB and the first RS in negative CG flashes with an exceptionally short channel.

4.4. Comparison With LBEs

According to their waveform characteristics, LBEs reported by Wu et al. (2014) can be considered as a subset of compact RSs. Pulses in Figures 2f and 2g are very similar to LBE waveforms. Wu et al. (2014) reported that almost all LBEs were located on land, so they speculated that LBEs were associated with tall grounded objects, which is not supported by the current study. The study by Wu et al. (2014) was based on an LF system far away from the Hokuriku region, so the location accuracy was relatively low. However, if we look at the locations of LBEs presented in their Figure 1, we can see that most LBEs were also located in mountain areas, in agreement with the result of the current study.

Another special feature of LBEs reported by Wu et al. (2014) is that LBEs are not preceded by other discharges. This is not supported by the current study either and may also be due to their remote observation which could not identify the small pulses before LBEs. In fact, if we look at the waveform example of an LBE in their Figure 3, we can clearly see several small pulses right before the LBE pulse; the duration might be around 100 μs, also consistent with the result of the current study.

The large bipolar pulse of LBEs is unlikely a fundamental feature; in fact, it is almost impossible to set quantitative criteria to identify LBEs from LF waveforms. This is clear by looking at Figure 2, which indicates that there is no clear dividing line between different types of waveforms. Therefore, it is more appropriate to consider LBEs as a subset of compact RSs in future studies.

5. Conclusion

In this study, we first analyzed special RSs in winter with predischarge durations (defined as the time difference between the RS pulse and the start of the flash) smaller than 1 ms. Such short time differences have never been reported for CG flashes in summer thunderstorms. We found that RSs with predischarge durations shorter and longer than 200 μs are systematically different. RSs with predischarge durations longer than 200 μs are generally similar to normal RSs, while those with durations shorter than 200 μs have some special characteristics not seen in normal RSs, including:

1. Pulse width, rise time, and fall time of the RS pulse all increase with increasing predischarge duration.
2. The rise time of the RS pulse is generally comparable to or larger than the fall time.
3. RS peak current increases with increasing predischarge duration.

These special RSs with predischarge durations shorter than 200 μs are named as compact RSs. Compact RSs along with preceding discharges are named as compact strokes. It is found that compact strokes mainly occur in mountain areas and none are on the sea. Almost all compact strokes lower negative charges. It is inferred that they are produced in small gaps between the main negative charge region in winter thunderstorms and mountain surfaces. Channel lengths of compact strokes are estimated to be shorter than 600 m with an average value of about 300 m, which are at least an order of magnitude shorter than those of normal RSs. The short channel is the reason for the short duration of preceding discharges.

It is likely that when winter thunderstorms develop to the mountain area, the altitude of the lower positive charge region is comparable to the elevation of the mountain surface. As a result, when thunderstorms are

over the mountain, the mountain surface and the near-surface space carry positive charges and are virtually the lower positive charge region of a normal tripole structure. Therefore, compact strokes are likely confined between the main negative charge region and the lower positive charge region. Small pulses preceding compact RSs are likely produced by the downward negative leader initiating from the lower edge of the main negative charge region and developing downward to the mountain surface. The leader corresponds to the PB stage, and there seems to be no stepped leader stage before compact RSs. Velocities of the leader are estimated to be about 3×10^6 m/s.

Appendix A: Estimating Stroke Peak Currents

Because fast antennas of the FALMA are not calibrated, we cannot directly estimate peak currents of RSs. However, using the data of the JLDN (e.g., Matsui et al., 2019), we can convert E-change peak magnitudes in DU to peak currents in kA for all detected strokes, including special strokes such as compact RSs that may not be identified by the JLDN. Here, we present a detailed description of the procedure for estimating peak currents used by the FALMA.

First, it is well known that the radiation field peak magnitude of RSs is inversely proportional to the distance. Therefore, peak magnitudes of RSs measured by any site can be range-normalized to 100 km using the following relationship:

$$E_{nor} = \frac{E \times D}{100} \tag{A1}$$

where E_{nor} is the E-change peak magnitude normalized to 100 km for any specific site, E is the E-change peak magnitude measured by the site, and D is the horizontal distance between the stroke and the site in km. Note that the above relationship is only true for radiation field, so the distance should not be too small. Here, we only consider strokes with distances to a specific site larger than 40 km. On the other hand, if the distance is too large, the location inaccuracy and propagation effects may become significant, so we only consider strokes with distances smaller than 200 km. Strokes saturating the site are also excluded.

Second, conversion coefficients between range-normalized peak magnitudes based on any two different sites are calculated. For example, the correlation between range-normalized peak magnitudes of site 0 and site 1 in Figure 5 are shown in Figure A1a. A total of 1,307 positive strokes and 1,017 negative strokes observed by both sites are used here, including some special strokes analyzed by the current study. As expected, range-normalized peak magnitudes of two different sites show excellent linear correlation. In this way, range-normalized peak magnitudes based on any site can be converted to the value based on site 0 with the following relationship:

$$E_0 = E_i \times \alpha_i \tag{A2}$$

where E_i is the range-normalized peak magnitude based on site i, E_0 is the peak magnitude converted to site 0, and α_i is the conversion coefficient between site i and site 0. The conversion coefficient is the slope of the regression line with zero intercept, but it is worth noting that in this case the slope does not change with or without zero intercept. For site 1 and site 0, for example, the conversion coefficient α_1 is 1.141 as shown in Figure A1a.

With the above two steps, we can convert peak magnitudes E of all strokes to the range-normalized value based on site 0 (E_0), which is a direct measure of the stroke peak current and can be compared directly for different strokes.

Finally, the conversion coefficient between E_0 and peak currents reported by JLDN is calculated. Because the JLDN data are very expensive, we only purchased the data for a 4-h period with high lightning frequency to do the calculation. For any RS reported by the JLDN, we search in our data set strokes with horizontal distances smaller than 1 km and time differences smaller than 0.5 ms. If multiple strokes are found, the stroke with the smallest time difference is selected. A total of 159 pairs are found, represented by red and blue dots in Figure A1b. The black dotted line is the linear regression line with zero intercept. There are apparently some mismatches in Figure A1b, so we exclude 10% (16) pairs that have largest distances from the regression line. These pairs are shown as blue dots. The linear regression with zero intercept is made

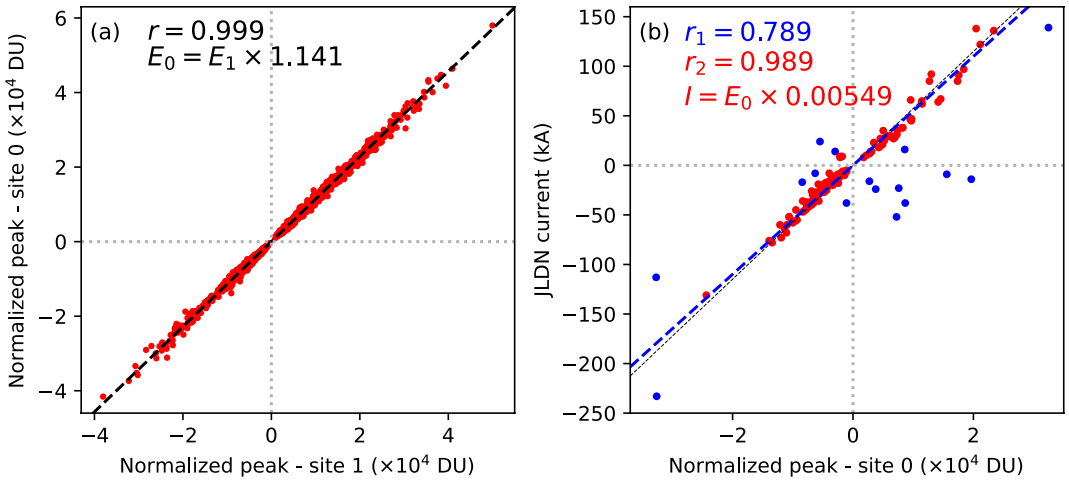

Figure A1. (a) Correlation between normalized peak magnitudes calculated based on site 0 and site 1. r is the correlation coefficient. (b) Correlation between normalized peak magnitudes of site 0 and peak currents reported by JLDN. The black dotted line is the regression line for all sources, and the correlation coefficient is r_1. The blue dashed line is the regression line for red sources, and the correlation coefficient is r_2. Locations of site 0 and site 1 can be found in Figure 5.

again for the remaining red dots, and the slope of the regression line is treated as the conversion coefficient. In this way, the normalized peak magnitude in DU can be converted to the peak current in kA with the following relationship:

$$I = E_0 \times \beta \tag{A3}$$

where β is the conversion coefficient and equals to 0.00549 as shown in Figure A1b.

With this procedure, peak E-change magnitudes measured by fast antennas can be converted to peak currents in kA for all strokes observed by the FALMA.

Data Availability Statement

Data for this study can be found online at http://doi.org/10.5281/zenodo.4760728.

Acknowledgments
This work was supported by the Ministry of Education, Culture, Sports, Science, and Technology of Japan (Grants 18K13618, 20H02129, and 21K03681).

References

Azadifar, M., Rubinstein, M., Rachidi, F., Rakov, V. A., Diendorfer, G., Schulz, W., & Pavanello, D. (2019). A study of a large bipolar lightning event observed at the Säntis tower. *IEEE Transactions on Electromagnetic Compatibility*, *61*(3), 796–806. https://doi.org/10.1109/TEMC.2019.2913220

Beasley, W., Uman, M. A., & Rustan, P. L., Jr. (1982). Electric fields preceding cloud-to-ground lightning flashes. *Journal of Geophysical Research: Oceans*, *87*(C7), 4883–4902. https://doi.org/10.1029/JC087iC07p04883

Bitzer, P. M., Christian, H. J., Stewart, M., Burchfield, J., Podgorny, S., Corredor, D., et al. (2013). Characterization and applications of vlf/lf source locations from lightning using the Huntsville Alabama Marx meter array. *Journal of Geophysical Research: Atmospheres*, *118*(8), 3120–3138. https://doi.org/10.1002/jgrd.50271

Brook, M. (1992). Breakdown electric fields in winter storms. *Journal of Atmospheric Electricity*, *12*(1), 47–52. https://doi.org/10.1541/jae.12.47

Clarence, N. D., & Malan, D. J. (1957). Preliminary discharge processes in lightning flashes to ground. *Quarterly Journal of the Royal Meteorological Society*, *83*(356), 161–172. https://doi.org/10.1002/qj.49708335603

Cummer, S. A., Lyu, F., Krehbiel, P. R., & William, R. (2020). A high peak current, negative polarity lightning process possibly associated with TGFs. In *AGU Fall Meeting Abstracts* (Vol. 2020, pp. AE013–01).

Gomes, C., Cooray, V., & Jayaratne, C. (1998). Comparison of preliminary breakdown pulses observed in Sweden and in Sri Lanka. *Journal of Atmospheric and Solar-Terrestrial Physics*, *60*(10), 975–979. https://doi.org/10.1016/S1364-6826(98)00007-8

Goto, Y., & Narita, K. (1995). Electrical characteristics of winter lightning. *Journal of Atmospheric and Terrestrial Physics*, *57*(5), 449–458. (URSI XXIVth General Assembly). https://doi.org/10.1016/0021-9169(94)00072-V

Ishii, M., & Saito, M. (2009). Lightning electric field characteristics associated with transmission-line faults in winter. *IEEE Transactions on Electromagnetic Compatibility*, *51*(3), 459–465. https://doi.org/10.1109/temc.2009.2025496

Kolmašová, I., Santolík, O., Farges, T., Rison, W., Lán, R., & Uhlíř, L. (2014). Properties of the unusually short pulse sequences occurring prior to the first strokes of negative cloud-to-ground lightning flashes. *Geophysical Research Letters*, *41*(14), 5316–5324. https://doi.org/10.1002/2014GL060913

Lin, Y. T., Uman, M. A., Tiller, J. A., Brantley, R. D., Beasley, W. H., Krider, E. P., & Weidman, C. D. (1979). Characterization of lightning return stroke electric and magnetic fields from simultaneous two-station measurements. *Journal of Geophysical Research*, *84*(C10), 6307–6314. https://doi.org/10.1029/JC084iC10p06307

Marshall, T., Stolzenburg, M., Karunarathne, S., Cummer, S., Lu, G., Betz, H.-D., et al. (2013). Initial breakdown pulses in intracloud lightning flashes and their relation to terrestrial gamma ray flashes. *Journal of Geophysical Research: Atmospheres*, *118*(19), 10907–10925. https://doi.org/10.1002/jgrd.50866

Matsui, M., Michishita, K., & Yokoyama, S. (2019). Characteristics of negative flashes with multiple ground strike points located by the Japanese lightning detection network. *IEEE Transactions on Electromagnetic Compatibility*, *61*(3), 751–758. https://doi.org/10.1109/TEMC.2019.2913661

Mecikalski, R. M., & Carey, L. D. (2017). Lightning characteristics relative to radar, altitude and temperature for a multicell, MCS and supercell over northern Alabama. *Atmospheric Research*, *191*, 128–140. https://doi.org/10.1016/j.atmosres.2017.03.001

Miyake, K., Suzuki, T., & Shinjou, K. (1992). Characteristics of winter lightning current on japan sea coast. *IEEE Transactions on Power Delivery*, *7*(3), 1450–1457. https://doi.org/10.1109/61.141864

Nag, A., & Cummins, K. L. (2017). Negative first stroke leader characteristics in cloud-to-ground lightning over land and ocean. *Geophysical Research Letters*, *44*(4), 1973–1980. https://doi.org/10.1002/2016GL072270

Nag, A., DeCarlo, B. A., & Rakov, V. A. (2009). Analysis of microsecond- and submicrosecond-scale electric field pulses produced by cloud and ground lightning discharges. *Atmospheric Research*, *91*(2), 316–325. https://doi.org/10.1016/j.atmosres.2008.01.014

Rakov, V. A., & Uman, M. A. (2003). *Lightning: Physics and effects* (p. 143). Cambridge University Press.

Shi, D., Wang, D., Wu, T., & Takagi, N. (2019a). Correlation between the first return stroke of negative cg lightning and its preceding discharge processes. *Journal of Geophysical Research: Atmospheres*, *124*(15), 8501–8510. https://doi.org/10.1029/2019JD030593

Shi, D., Wang, D., Wu, T., & Takagi, N. (2019b). Temporal and spatial characteristics of preliminary breakdown pulses in intracloud lightning flashes. *Journal of Geophysical Research: Atmospheres*, *124*(23), 12901–12914. https://doi.org/10.1029/2019JD031130

Stolzenburg, M., & Marshall, T. C. (2008). Charge structure and dynamics in thunderstorms. *Space Science Reviews*, *137*(1-4), 355–372. https://doi.org/10.1007/978-0-387-87664-1_23

Thomas, R. J., Krehbiel, P. R., Rison, W., Hunyady, S. J., Winn, W. P., Hamlin, T., & Harlin, J. (2004). Accuracy of the lightning mapping array. *Journal of Geophysical Research*, *109*(D14), 1–2. https://doi.org/10.1029/2004JD004549

Wada, Y., Enoto, T., Nakamura, Y., Morimoto, T., Sato, M., Ushio, T., et al. (2020). High peak-current lightning discharges associated with downward terrestrial gamma-ray flashes. *Journal of Geophysical Research: Atmospheres*, *125*(4), e2019JD031730. https://doi.org/10.1029/2019JD031730

Wang, D., Zheng, D., Wu, T., & Takagi, N. (2021). Winter positive cloud-to-ground lightning flashes observed by LMA in Japan. *IEEJ Transactions on Electrical and Electronic Engineering*, *16*(3), 402–411. https://doi.org/10.1002/tee.23310

Williams, E. R. (1989). The tripole structure of thunderstorms. *Journal of Geophysical Research: Atmospheres*, *94*(D11), 13151–13167. https://doi.org/10.1029/JD094iD11p13151

Wu, T., Takayanagi, Y., Funaki, T., Yoshida, S., Ushio, T., Kawasaki, Z.-I., et al. (2013). Preliminary breakdown pulses of cloud-to-ground lightning in winter thunderstorms in Japan. *Journal of Atmospheric and Solar-Terrestrial Physics*, *102*, 91–98. https://doi.org/10.1016/j.jastp.2013.05.014

Wu, T., Wang, D., & Takagi, N. (2018). Lightning mapping with an array of fast antennas. *Geophysical Research Letters*, *45*(8), 3698–3705. https://doi.org/10.1002/2018GL077628

Wu, T., Wang, D., & Takagi, N. (2020a). Multiple-stroke positive cloud-to-ground lightning observed by the falma in winter thunderstorms in japan. *Journal of Geophysical Research: Atmospheres*, *125*(20), e2020JD033039. https://doi.org/10.1029/2020JD033039

Wu, T., Wang, D., & Takagi, N. (2020b). Upward negative leaders in positive upward lightning in winter: Propagation velocities, electric field change waveforms, and triggering mechanism. *Journal of Geophysical Research: Atmospheres*, *125*(16), e2020JD032851. https://doi.org/10.1029/2020JD032851

Wu, T., Yoshida, S., Akiyama, Y., Stock, M., Ushio, T., & Kawasaki, Z. (2015). Preliminary breakdown of intracloud lightning: Initiation altitude, propagation speed, pulse train characteristics, and step length estimation. *Journal of Geophysical Research: Atmospheres*, *120*(18), 9071–9086. https://doi.org/10.1002/2015JD023546

Wu, T., Yoshida, S., Ushio, T., Kawasaki, Z., Takayanagi, Y., & Wang, D. (2014). Large bipolar lightning discharge events in winter thunderstorms in Japan. *Journal of Geophysical Research: Atmospheres*, *119*(2), 555–566. https://doi.org/10.1002/2013JD020369

Yoshida, S., Wu, T., Ushio, T., Kusunoki, K., & Nakamura, Y. (2014). Initial results of lf sensor network for lightning observation and characteristics of lightning emission in lf band. *Journal of Geophysical Research: Atmospheres*, *119*(21), 12034–12051. https://doi.org/10.1002/2014JD022065

Zhu, Y., Rakov, V., & Tran, M. (2017). Optical and electric field signatures of lightning interaction with a 257-m tall tower in Florida. *Electric Power Systems Research*, *153*, 128–137. https://doi.org/10.1016/j.epsr.2016.08.036

Zhu, Y., Rakov, V. A., Mallick, S., & Tran, M. D. (2015). Characterization of negative cloud-to-ground lightning in Florida. *Journal of Atmospheric and Solar-Terrestrial Physics*, *136*, 8–15. https://doi.org/10.1016/j.jastp.2015.08.006